# Finite Element Model Of A Helical Swimming Robot In COMSOL Multiphysics®

Miguel A. López, José Emilio Traver, Cristina Nuevo-Gallardo, Paloma Rodríguez-Díaz, Inés Tejado, Blas M. Vinagre.
University of Extremadura, Badajoz, Ex, Spain

## Abstract

**This work presents a small helical swimmer model in a low Reynolds number (*Re*) environment governed by the equation of motion for Stokes flow in COMSOL Multiphysics®. The entity, a few centimetres helical robot, is located inside of a pipe full of silicone oil, where the forces caused by the robot's rotation rate Ω and the axial velocity *U* are studied. By means of the COMSOL Multiphysics® Computational Fluid Dynamics (CFD) Module, it is possible to implement a laminar flow in which inertial terms are neglected (Stokes flow). Within this framework, the work is divided into two independent parts: a first one in which the longitudinal motion is simulated, and a second one in which it is performed the rotation of the helix. Results are compared with the Resistive Force Theory (RFT) based on the premise that, in low *Re* environments, force and torque contributions caused by the robot's axial velocity *U* and rotation rate Ω are additive. The input flow emulates the longitudinal motion of the robot in order to obtain the drag forces caused by fluid resistance. The motion rate study uses the moving mesh to emulate the spinning of the helix. To lighten the computational cost of the model, a frozen rotor approximation is implemented to estimate the forces and torque generated by rotation. By means of this model, it is possible to study the impact of robot's geometry parameters on swimming performance, like the pitch $\lambda$, the length $L$ and the exponential envelope. Therefore, different propeller geometry combinations have been studied in this work. From an efficiency point of view, an optimal value is obtained when $\lambda = 7R$, where $R$ is the radius of the helix. Likewise, the linear dependence of hydrodynamics forces regarding the normalized length of the helix is verified. Finally, results reveal that the COMSOL Multiphysics® model is more appropriate than RFT in a design process, since it can estimate the robot performance, even for complex geometries, in a standalone simulation.**

## 1. Introduction

Microscale technology is receiving much more attention in the recent years since it is potentially suitable for very small spaces, and, therefore, very useful for biomedical applications in a less invasive way (Nelson, Kaliakatsos and Abbott 2010). Some of them are focused on an accurate distribution of drugs or the manipulation and interaction with tiny entities in the environment (Boguet 2015, Diller and Sitti 2013). To accomplish this goal, it is necessary to be familiarised with the microscale hydrodynamics and the low Reynolds number ($Re$) regime. In this context, Purcell introduced the swimming efficiency by a rotating helical flagellum in low $Re$ (Purcell 1997), obtaining a linear relationship between the forces $F$ and torque $N$ and its linear $U$ and rotational speed $\Omega$ by means of the resistive matrix (He-Peng, et al. 2014). This matrix is proportional to the fluid viscosity and depend on the helix shape.

The main purpose of a helical propeller is to boost microscale entities in a non-invasive surgical procedure. One approach to understand how the shape of these propellers affect swimming efficiency is through the slender-body theory (SBT), which calculates the flow field around the helix by means of the Stokeslet and its derivates, a singular point force embedded in a Stokes flow along the centreline of the flagellum (J.J.L.Higdon 1979). The limitation of this theory is the necessity of evaluating intractable integrals constantly to determine the force on each point. In (Cortez, Fauci y Medovikov 2005), it is presented the method of the regularized Stokeslet for computing a Stokes flow leaded by forces distributed along material points, a simple discretization of the SBT for $N$ stokeslets located along the surface of the solid body. To simplify the SBT, (Gray and Hancock 1955, Lighthill 1979) introduced the Resistive Force Theory (RFT) by considering each segment of the flagellum represented by the Stokeslet and its derivates as an independent slender rod. Through this simplification, it is possible to estimate the resistive matrix coefficients in first instance and still understand how the helix shape will influence its swimming efficiency.

Another approach to study the swimming efficiency of a helix is by means of simple experiments. In (Xu, et al. 2015), it is analysed the impact of helix geometry in swimming efficiency through a design of experiments, a test series in which changes are made in the geometrical parameters and the effects on the response variables are measured. In (Rodenborn, et al. 2013) it is compared the slender-body theory with the RFT in conjunction with experimental results. Finally, fundamental properties of bacterial propulsion are determined by measuring the force required to hold the bacterium *Escherichia coli* in an optical trap in (Chattopadhyay, et al. 2006).

These related works analyse the mechanism of swimming either from a theoretical and an experimental point of view. Therefore, and based on the state of art, there is a gap in simulation and analysis of how the helix geometry affects the swimming performance, especially in the case of one parameter depending on another, e.g., a variable helix radius or a variable pitch along the length of the propeller. Within this framework, the main purpose of this work is to implement a helical propeller model in COMSOL Multiphysics® to study how changes in geometrical parameters influence swimming efficiency in a low $Re$ environment. To accomplish this goal, three parameters are studied: the pitch $\lambda$, the length $L$ and an exponential envelope factor shape $\alpha$. The propeller is based on the cardiovascular system platform presented in (Nuevo-Gallardo, et al. 2019) as future experiments will be conducted on this environment.

The document is organised as follows. Section 2 introduces common properties of microscale hydrodynamics, *Re* and Stokes equations, widely used in this area. Section 3 presents the model in COMSOL Multiphysics®. Section 4 shows the three test parameters studied and the simulations results. Finally, the conclusions of this work are drawn in Section 5.

## 2. Hydrodynamics in low Re regime

Microscale hydrodynamics requires to work in low *Re* environment. This value captures the flow characteristic regime, being expressed as:

$$Re = \frac{vL\rho}{\mu} \tag{1}$$

where $v$ is the maximum fluid velocity, $L$ is the characteristic length, and $\rho$ and $\mu$ are the density and the dynamic viscosity of the fluid, respectively.

**Table 1:** Blood properties of the cardiovascular system.

| Property | Value | Units |
|---|---|---|
| Blood Density | 1070 | kg/m$^3$ |
| Blood Dynamic Viscosity | $3.5\ 10^{-3}$ | Pa·s |
| Output Heart Flow | $6\ 10^{-4}$ | m$^3$/s |
| Silicone Oil Density | 964 | kg/m$^3$ |
| Silicone Oil Dynamic Viscosity | 0.0964 | Pa·s |

For applications with micro entities inside of the human body, the corresponding value of $Re$ must be calculated using blood properties such as the ones given in Table 1. With these values, a low $Re$ number environment is achieved. In contrast, for a robot of the order of millimetres or centimetres, it is necessary to increase the viscosity of the fluid to keep a low $Re$ number, and consequently, achieve an equivalent environment. For instance, it can be used silicone oil instead of blood (see Table 1). A low $Re$ number implies that viscosity predominates over inertia, affecting the dynamics of fluid particles (Happel and Brenner 1983). Therefore, Navier-Stokes and continuity equations for a Newtonian and an incompressible fluid are reduced to the Stokes equation:

$$\begin{gathered} -\nabla p + \mu \nabla^2 u = 0 \\ \nabla \cdot u = 0 \end{gathered} \tag{2}$$

where $u$ is the flow velocity, $\nabla p$ is the gradient of pressure and $\nabla$ is the nabla operator. Since equation (2) is a linear and a time-independent expression, the relation between kinetics and kinematics is also linear. Thus, if the solid body is subject to an external force $F$ and/or a torque $N$, it will move with a linear velocity $U$ and a rotation rate $\Omega$, satisfying the abovementioned resistive matrix:

$$\begin{bmatrix} F \\ N \end{bmatrix} = \begin{bmatrix} A & B \\ B^T & C \end{bmatrix} \cdot \begin{bmatrix} U \\ \Omega \end{bmatrix} \tag{3}$$

The terms of equation (3) rely purely on the geometrical parameters of the swimmer. For instance, the resistive matrix of an ellipsoid cell body will be diagonal since it can not propel itself. In most cases, the geometry makes impossible to calculate matrix coefficients analytically. Nevertheless, for a straightforward helical shape, these can be estimated from RFT by:

$$\begin{aligned} A &= (\xi_\perp \sin^2\theta + \xi_{/\!/} \cos^2\theta)\frac{L}{\cos\theta} \\ B &= RL(\xi_\perp - \xi_{/\!/})\sin\theta \\ C &= R^2(\xi_\perp \cos^2\theta + \xi_{/\!/} \sin^2\theta)\frac{L}{\cos\theta} \end{aligned} \tag{4}$$

where $\theta = \tan^{-1}(\frac{2\pi R}{\lambda})$, $R$ and $L$ are the radius and the length of the propeller, and $\xi_\perp$ and $\xi_{/\!/}$ are the Gray and Hancock's drag coefficients, respectively, given as follows:

$$\begin{aligned} \xi_\perp &= \frac{2\pi\mu}{\ln\left(\frac{2\lambda}{a}\right) - \frac{1}{2}} \\ \xi_{/\!/} &= \frac{4\pi\mu}{\ln\left(\frac{2\lambda}{a}\right) + \frac{1}{2}} \end{aligned} \tag{5}$$

where $a$ is the filament radius and $\lambda$ is the pitch of the propeller. In order to find which terms of equation (3) are most suitable for an optimal shape, it is convenient to use the next efficiency ratio, see (He-Peng, et al. 2014):

$$\epsilon = \frac{B^2}{4AC} \cdot 100 \tag{6}$$

Drag and thrust can be easily computed in COMSOL Multiphysics® through the integral of total stress parallel to the helix, i.e.:

$$F_x = \int_s \sigma_x dS \tag{7}$$

while torque can be obtained by integration of the vectorial product of the stress (8), i.e.:

$$N_x = \int_s (z\sigma_y - y\sigma_z) dS \tag{8}$$

where $\sigma_x$, $\sigma_y$ and $\sigma_z$ are the stress in the x, y and z directions and $dS$ is the surface differential. Through equations (7) and (8), it is possible to estimate coefficients of equation (3) numerically as:

$$A = \frac{F_x}{U_{sim}} \tag{9}$$

$$B = \frac{F_x}{\Omega} \tag{10}$$

$$C = \frac{N_x}{\Omega} \tag{11}$$

## 3. Modelling in COMSOL Multiphysics®

A low Re number implies that linear and rotational speed contributions are additive (see equation (3)). Therefore, the work is divided into two independent simulations: a first one to emulate longitudinal motion, and a second one to perform rotation. For this purpose, a helical swimming robot inside of a lumen has been developed in COMSOL Multiphysics® to analyse how changes in the geometry of the helix affects its dynamics within a fluid.

This model emulates the lumen of a human body by means of two control regions differentiated by two cylinders: a surrounding fluid close to a helix located in the centre of the model and the remaining fluid inside the lumen. This distinction simplifies the helix motion, since, as will be commented later, a moving mesh will be attached to this inner control region.

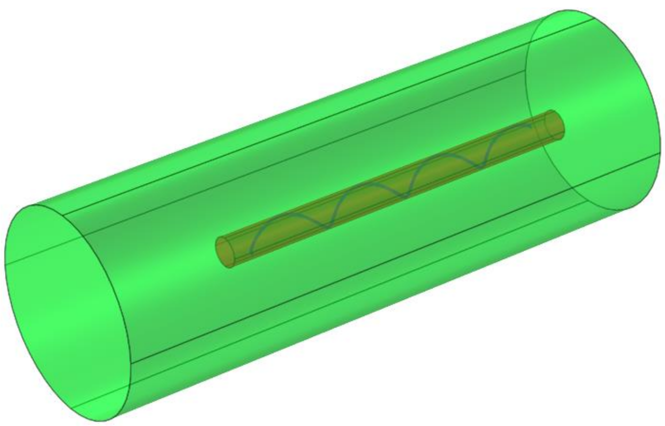

**Figure 1** Model of the helical swimming robot within a lumen flow environment in COMSOL Multiphysics®.

Regarding the helix geometry, its design is based on the schematic shown in Figure 2.

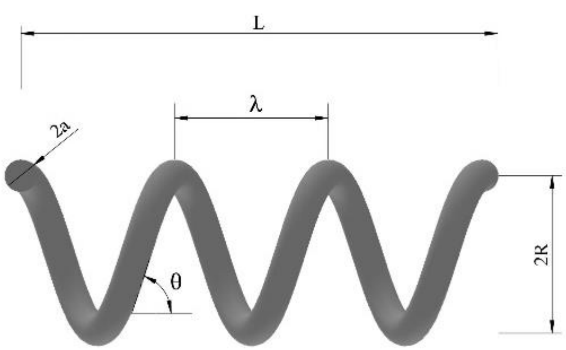


**Figure 2.** Schematic of a helical flagellum.

with radius $R$, pitch $\lambda$, length $L$, filament radius $a$ and pitch angle $\theta$. Parameters $R$ and $a$ are constant and are shown in Table 2, as well as, the linear and angular speed of the robot and the lumen radius. It is important to remark that, since experiments will be carried out on the cardiovascular system platform designed in (Nuevo-Gallardo, et al. 2019), the set-up and its dimensions are adapted to the size of this environment. Especially, the size of the lumen, which matches the size of the pipes used in the platform.

Likewise, as commented in the introduction of this document, the influence in swimming efficiency of an exponential envelope will be studied. In helixes, there is a geometrical parameter related to the function that envelops the own helix, as illustrated in Figure 3. In this work , an exponential envelope of the form $1 - e^{-\alpha s^2}$ is modelled, where $s$ defines the helix coordinates and $\alpha$ is a constant which defines how fast the envelope approaches to 1. To do so, three parametric functions of this type are included in the model and swept along the axial axis.

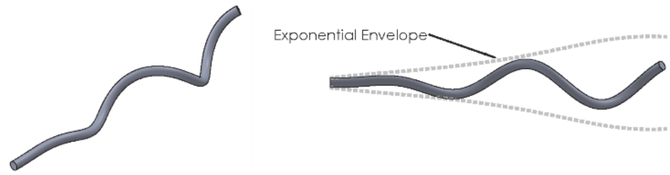


**Figure 3.** Isometric and front view of a propeller with the exponential envelope $1 - e^{-\alpha s^2}$ applied over the helix radius regarding $\alpha$.

A laminar fluid is implemented by means of the Computational Fluid Dynamics (CFD) Module for each part. The lumen is filled with silicon oil to ensure that a low $Re$ condition is achieved. Thus, it is possible to emulate a Stokes flow in which inertial terms are rejected. Furthermore, a non-slip condition is attached to the surface of the helix and the surface of the lumen. This setting ensures that the fluid will have zero velocity relative to these boundaries. The longitudinal motion of this propeller is achieved by including an input/output flow into the lumen. In this case, the input flow velocity is that on the platform, being equivalent to the mean blood velocity into the ascending aorta to reproduce the conditions given inside the cardiovascular system of the human body (Nuevo-Gallardo, et al. 2019). The CFD Module allows to implement this part very easily, as shown in Figure 4.

Likewise, the helix rotation requires the addition of a moving mesh. In this case, a general velocity $\Omega$ moving mesh is implemented and attached to the inner cylinder as a first approach of rotation. The frozen rotor approximation is included in simulation to reduce the execution time significantly. With this setting, the helix does not rotate during the execution, however, rotation and associated momentum terms are imparted to the flow. Therefore, it is possible to obtain a pseudo-steady-state condition of the helix rotation dynamics.

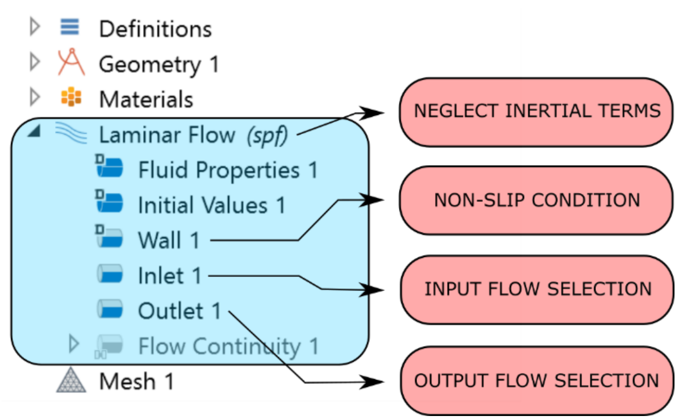


**Figure 4.** Laminar flow COMSOL Multiphysics® drop-down menu.

**Table 2:** Geometrical and fluid parameters used in simulation.

| **Property** | | **Value** | **Units** |
|---|---|---|---|
| Lumen Radius | $(R_L)$ | 5 | cm |
| Filament Radius | $(a)$ | 0.4 | mm |
| Helix Radius | $(R)$ | 6.4 | mm |
| Angular Velocity | $(\Omega)$ | 6.2832 | rad/s |
| Linear Velocity | $(U)$ | 0.0670 | m/s |

## 4. Simulations and results

To study how changes in geometrical parameters influence swimming performance of the helical robot, an efficiency study has been carried out on the model described in the previous section modifying the following three parameters:

1. Helix pitch $\lambda$.
2. Helix length $L$.
3. Helix envelope factor $\alpha$.

In particular, the developed model allows to estimate terms of equation (3) by means of equations (9)-(11). Simulated results are compared in all the cases with RFT through MATLAB. The geometrical values used in simulation are given in Table 3. Results of normalized thrust, drag, torque and efficiency are shown next.

**Table 3:** Geometrical parameters range used for the simulation and for the RFT. Study 1, 2 and 3 refer to the pitch $\lambda$, length $L$ and the envelope $\alpha$ cases, respectively.

| | **Parameter range** | | |
|---|---|---|---|
| **Study** | $\boldsymbol{\lambda}$ | $\boldsymbol{L}$ | $\boldsymbol{\alpha}$ |
| 1 | $R - 20R$ | $5R, 10R, 15R, 20R, 25R$ | – |
| 2 | $7R$ | $R - 20R$ | – |
| 3 | $7R$ | $5R, 10R, 15R$ | $0.1 - 0.1 \cdot 10^{-2}$ |

### 4.1. Study 1: Influence of Helix Pitch

To check how pitch $\lambda$ affects the hydrodynamics forces and the efficiency, a parametric sweep study is considered for parameter $\lambda$. In this case, a normalized $\lambda$ varies from $R$ to $20R$ with a step of $R/2$. Likewise, five different values of helix's lengths $L$ are simulated. In this and all subsequent cases, when the helix rotates at speed of $\Omega$, thrust is estimated computing equation (7) and torque computing equation (8). In the same way, equation (7) also allows to estimate drag when the helix moves at a linear speed $U$. These simulated results for thrust, drag and torque are compared with the obtained applying RFT (equations (3) – (5)).

As shown in Figure 5(a), discrepancy in thrust is significant. RFT seems to be a good approach to estimate the hydrodynamics forces generated by a helical swimming robot for large values of $\lambda$; nevertheless, as pitch approaches to zero, discrepancies between RFT and simulation become too large.

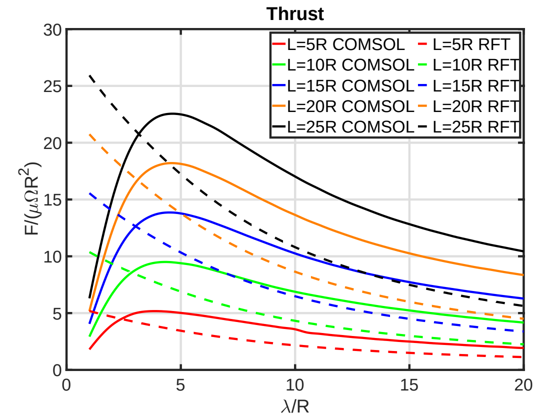


**(a)**

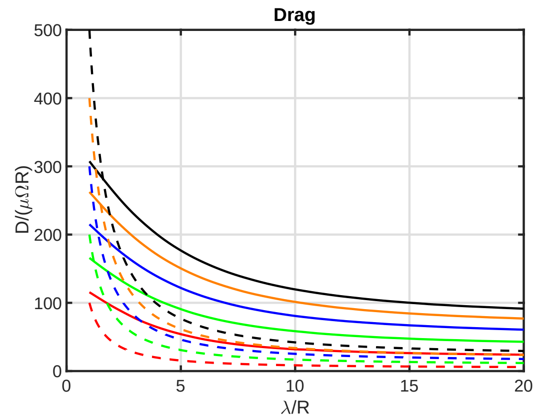


**(b)**

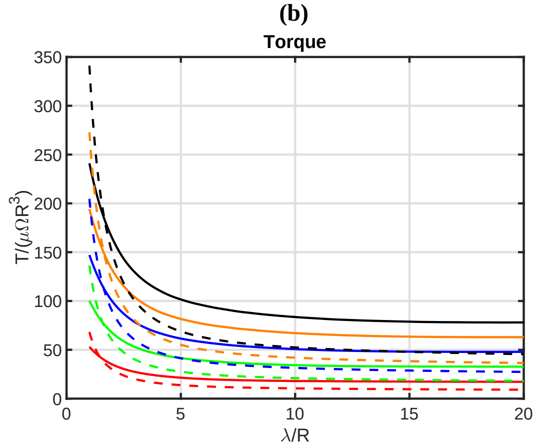


**(c)**

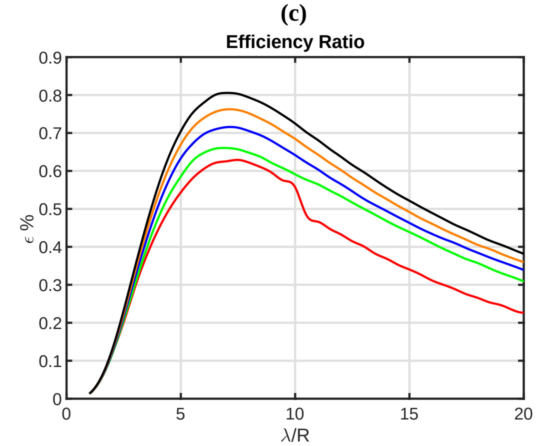


**(d)**

**Figure 5.** Normalized thrust (a), drag (b) and torque (c) generated by the helix as a function of normalized $\lambda$ regarding the radius $R$. Efficiency (d) shows an optimal point when $\lambda = 7R$.

Differences in drag and torque (see Figure(b) and (c)) are less noticeable. As the pitch approaches to zero, drag and torque increase exponentially. If a fixed torque ratio is associated to a helix turn, the greater number of turns, the greater the torque generated. However, it will also increase the drag associated to the robot. And in what efficiency in swimming is concerned (see Figure 5(d)), it can be seen that there is an optimal when $\lambda = 7R$, but being greater as the length of the helix increases. These results show that, for sizes close to the size of a bacterium, COMSOL Multiphysics seems to be a better approach to estimate thrust, drag and torque generated by a helical swimming robot.

### 4.2. Influence of helix length

The second study analyses how changes in the length $L$ of the helix affect swimming performance. Through RFT it can be said that there should be a linear dependence between the hydrodynamics forces and the helix length $L$, since it multiplies the factors of the resistive matrix (equation (4)) directly. In this study, pitch matches the optimal value obtained previously $\lambda = 7R$. Normalized length $L$ varies from $R$ to $20R$.

Figure 6 illustrates normalized thrust, drag and torque for normalized L with respect to the radius $R$ in simulation and applying RFT. As can be observed, there exist significant differences between RFT and the results obtained with COMSOL Multiphysics®, probably because Gray and Hancock's drag coefficients are not the best approach for the longitudinal and the perpendicular drag of the helix. Nevertheless, the linear dependence is verified in simulation for thrust and torque, and somehow for drag. Conclusions drawn regarding the length $L$ of the helix are straightforward: thrust, drag and torque will increase as $L$ increases.

It is important to remark that, due to convergence problems with the simulated model, efficiency could not be calculated correctly. However, all the hydrodynamics forces can be approximated by a linear function, and consequently, it is foreseeable that efficiency will be a constant value regarding $L$, as long as it was defined as shown in equation (6). Therefore, $L$ will be an important parameter to be taken into account depending on the application, but rather than being a crucial factor to take into account when studying the swimming efficiency of the robot.

### 4.3. Influence of helix envelope factor

In this last study, the influence of the envelope shape of the helix on the swimming efficiency is analysed for three different helix lengths. With this configuration, it is possible to modify the value of $\alpha$ and simulate different shapes. As shown in Figure 7, efficiency decays as the value of $\alpha/R$ comes close to zero (actually, for values lower than $2\alpha/R$), but grows slightly as $\alpha/R$ increases for a value higher than $2\alpha/R$, keeping almost constant. Therefore, there is no advantage in using this configuration for the time being. In case of using a body head, if the radius of the head matches the radius of the helix, the drawback in efficiency would probably be eliminated; since, in the natural motion of the robot, the head would cover the helix until it will reach its original shape.

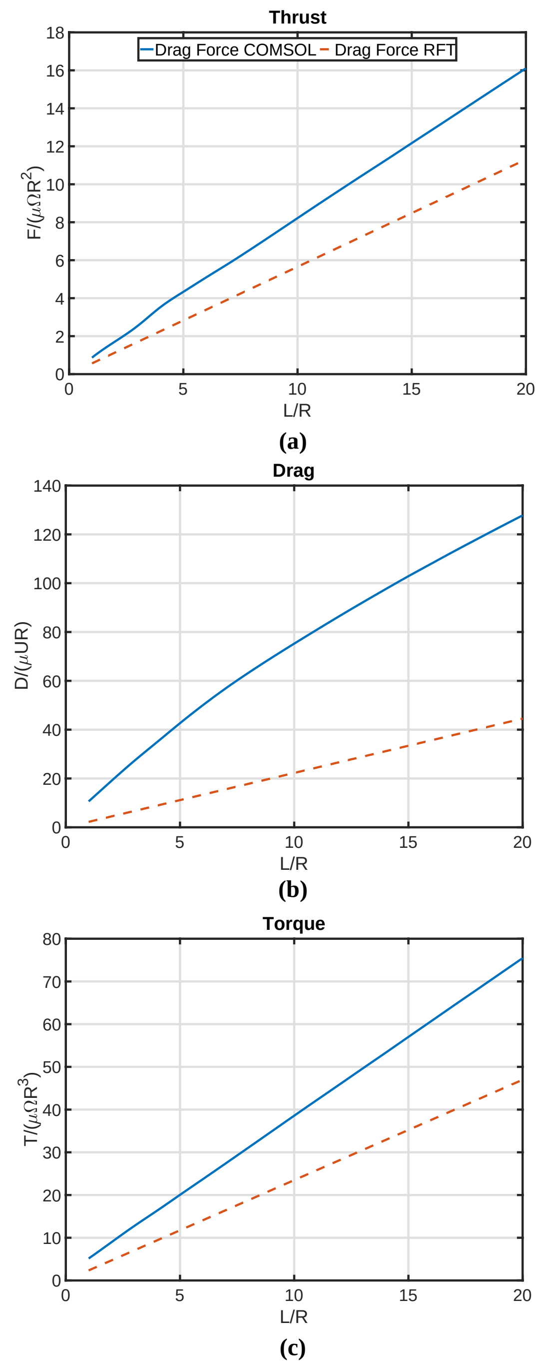


**Figure 6.** Normalized thrust (a), drag (b) and torque (c) generated by the helix as a function of normalized $L$ regarding the radius $R$.

## 5. Conclusions

In this work, a robot helix model propelled in a fluid has been implemented in COMSOL Multiphysics® to study how changes in geometrical parameters influence swimming efficiency. Through this model, a numerical RFT equivalent was obtained, in which the relationship between the linear and rotational speed, and the hydrodynamic forces, was estimated. Drag and thrust were obtained by integration of the stress parallel to the helix and torque by integration of the vectorial product of the stress perpendicular to the axial direction. In particular, the influence of three different aspects were studied: pitch $\lambda$, length $L$ and the shape of the helix envelope. An optimal in efficiency was obtained when $\lambda = 7R$, being greater

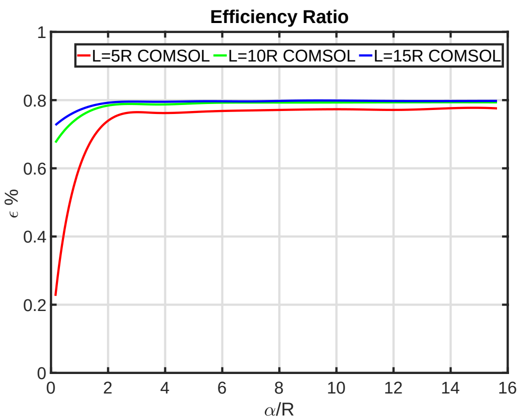


**Figure 7.** Swimming efficiency as a function of normalized $\alpha/R$

as the length of the helix increases. The linear dependence of hydrodynamic forces regarding the length of the helix was verified. However, due to convergence problems with the simulation, efficiency results could not be estimated for changes in length $L$. A helix model with an exponential envelope was also implemented. It is concluded that this shape was not convenient to maintain swimming efficiency.

Future works will go in different directions. Firstly, it would be interesting to manufacture milli and micro robots based on the conclusions drawn from these simulations. It will be necessary to test these prototypes on the cardiovascular system platform as commented before. Moreover, future approaches will also include the body head of the robot in the COMSOL Multiphysics® model. It would be also required to investigate how the efficiency is affected by the length of the helix in more detail. Likewise, it will be necessary to relate the power consumption and the efficiency, and to study the performance of new and ground-breaking designs, which will allow to increase the swimming efficiency.

## References


1. Nelson, Bradley J., Ioannis K. Kaliakatsos, and Jake J. Abbott. Microrobots for minimally invasive medicine. *Annual Review of Biomedical Engineering*, **12**, 55-85 (2010).
2. Boguet, Robert. Miniature and microrobots: A review of recent developments. *Industrial Robot: An International Journal*, **42**, 98-102 (2105).
3. Diller, Eric, and Metin Sitti. Micro-Scale Mobile Robotics. *Foundations and Trends® in Robotics*, **2**, 143-259 (2013).
4. Purcell, Edward M. The efficiency of propulsion by a rotating flagellum. *Proceedings of the National Academy of Sciences*, **94**, 11307-11311 (1997).
5. He-Peng, Zhang, Liu Bin, Bruce Rodenborn, and Harry L.Swinney. Propulsive matrix of a helical flagellum. *Chinese Physics B*, **23**, 114703 (2014).
6. J.J.L.Higdon. A hydrodynamic analysis of flagellar propulsion. *Journal of Fluid Mechanics*, **90**, 685-711 (1979).
7. Cortez, Ricardo, Lisa Fauci, and Alexei Medovikov. The method of regularized Stokeslets in three dimensions: Analysis, validation, and application to helical swimming. *Physics of Fluids*, **17**, 031504 (2005).
8. Gray, J, and G.J. Hancock. The propulsion of Sea-Urchin Spermatozoa. *Journal of Experimental Biology*, **32**, 802-814 (1995).
9. Lighthill, James. Flagellar Hydrodynamics. *Biophysical Journal*, **25**, 113-127 (1979).
10. Xu, Tiantian, Gilgueng Hwang, Nicolas Andreff, and Stéphane Régnier. Influence of geometry on swimming performance of helical swimmers using DoE. *Journal of Micro-Bio Robotics*, **11**, 57-66 (2015).
11. Rodenborn, B., C.-H. Chen, H. L. Swinney, B. Liu, and H. P. Zhang. Propulsion of microorganisms by a helical flagellum. *Proceedings of the National Academy of Sciences*, **110**, E338-E347 (2013).
12. Chattopadhyay, Suddhashil, Radu Moldovan, Chuck Yeung, and X. L. Wu. Swimming efficiency of bacterium Escherichia coli. *Proceedings of the National Academy of Sciences*, **103**, 13712-13717 (2006).
13. Nuevo-Gallardo, Cristina, José Emilio Emilio Traver, Inés Tejado, Javier Prieto-Arranz, Miguel A. López, and Blas M. Vinagre. Diseño en Solidworks de plataforma del sistema cardiovascular para ensayo de robots de navegación autónoma. *XL Jornadas de Automática*, 544-551 (2019).
14. Happel, John, and Howard Brenner. Low Reynolds number hydrodynamics. 2. Martinus Nijhoff Publishers, United States (1983).


## Acknowledgements

This work has been supported in part by the project IB18109 and the Consejería de Economía e Infraestructuras (Junta de Extremadura) under the grant ”Ayuda a Grupos de Investigación de Extremadura” (no. GR18159) and in part by the European Regional Development Fund ”A way to make Europe”.